

TVV and *TTP* couplings and related strong and electromagnetic decays of tensor mesons*

N. Levy, P. Singer, and S. Toaff

Department of Physics, Technion-Israel Institute of Technology, Haifa, Israel

(Received 29 October 1975)

Equations for *TVV* and *TTP* couplings are derived from dual amplitudes for the processes $P + V \rightarrow P + V$ and $P + T \rightarrow P + P$. The couplings are expressed in terms of other mesonic couplings, known from experiment. With the aid of these couplings we calculate the decay rates of $A_2 \rightarrow \omega\pi\pi$, $f \rightarrow \rho\pi\pi$, $K^{**} \rightarrow K^*\pi\pi$ and the electromagnetic decays $A_2, f \rightarrow V\gamma$, and $\gamma\gamma$. The calculated rates for $A_2 \rightarrow \omega\pi\pi$ and $f \rightarrow \rho\pi\pi$ are smaller (by about a factor of 4) than the average experimental data. This discrepancy is analyzed in terms of a consistent picture for all the decays studied in this paper.

I. INTRODUCTION

It has become evident during the last decade that a good phenomenological description of the strong and electromagnetic decays of pseudoscalar (P) and vector mesons (V) is achieved by the use of an effective Lagrangian (in the tree approximation), containing the strong VPP and VVP couplings.¹ With the aid of specific symmetry considerations concerning meson multiplets and couplings, and vector-meson dominance of the electromagnetic current, a whole variety of decays is thus described in terms of very few parameters (i.e., couplings and mixing angles). The large body of experimental data which has accumulated till now has led to the determination of these parameters at a fairly satisfactory level of accuracy.² A natural extension of this scheme is to include tensor-meson (T) decays. A first step was the description of their main decays (e.g., $f \rightarrow \pi\pi$, $K^{**} \rightarrow K\pi$, $A_2 \rightarrow \rho\pi, \eta\pi$) in terms of TPP and TVP couplings.²

In the present paper we investigate the yet scarcely known tensor-vector-vector (*TVV*) and tensor-tensor-pseudoscalar (*TTP*) couplings. We were partly motivated by the actuality of rare-modes detection, like the recent measurements^{3,4} of $A_2 \rightarrow \omega\pi\pi$ and $f \rightarrow 4\pi$ (which is partially $f \rightarrow \rho\pi\pi$). These decay modes, as well as many electromagnetic decays of tensor mesons, can be described with the aid of the above couplings.

The paper is divided as follows: in the second section we recapitulate a previously suggested dual model for $P + V \rightarrow P + V$ amplitudes from which we derive expressions for *TVV* couplings, including the case where the V 's are photons. A similar model for the $P + T \rightarrow P + P$ amplitudes serves to derive the *TTP* couplings. With the aid of these couplings we proceed in Sec. III to calculate the decays $A_2 \rightarrow \omega\pi\pi$ and $f \rightarrow \rho\pi\pi$. Generally our results are smaller by a factor of ~ 4 than the reported experimental averages. In confining ourselves to *TVV* and *TTP* vertices for the strong modes,

we did not include possible exchanges involving axial-vector mesons (e.g., A_1 and B) because of the uncertainty concerning the existence of some of the axial-vector mesons. Models which include the contribution of these mesons have been proposed in the literature. Several differential cross sections, which could distinguish between the present approach and the models based on axial-vector-meson exchange, are then displayed. The already existing data favor the *TVV* model. In Sec. IV we present the predictions of the model for electromagnetic decay rates of the type $T \rightarrow V\gamma$ and $T \rightarrow \gamma\gamma$, and compare them with the results obtained by other authors.

The last section includes a summary of our results and a discussion of the possible solution for the discrepancy between the calculated and observed $T \rightarrow VPP$ partial rates. The implications for the yet unobserved $K^{**} \rightarrow K^*\pi\pi$ mode [predicted to have a width of at least $\sim 0.6\Gamma(A_2 \rightarrow \omega\pi\pi)$], and for the electromagnetic decays are then noted.

Appendix A contains a list of the expressions we used for the various mesonic vertices and the values of coupling constants as determined from measured decay widths. Appendix B contains the definitions and the kinematics for $A_2 \rightarrow \pi\pi$ and the dynamical expressions of the invariant amplitudes on which the present calculation is based.

II. DUAL AMPLITUDES AND COUPLING-CONSTANT RELATIONS

In the detailed treatment of the $A_2 \rightarrow \omega\pi\pi$ and $f \rightarrow \rho\pi\pi$ decays, we shall want to include the contributions of resonances in the direct channel and particle exchanges in the crossed channels. This requires the knowledge of several tensor-meson couplings, namely the *TVV*, *TTP*, and *TVP*. Only the last one is known from a direct measurement. The first two are derived in this chapter from a theoretical model.

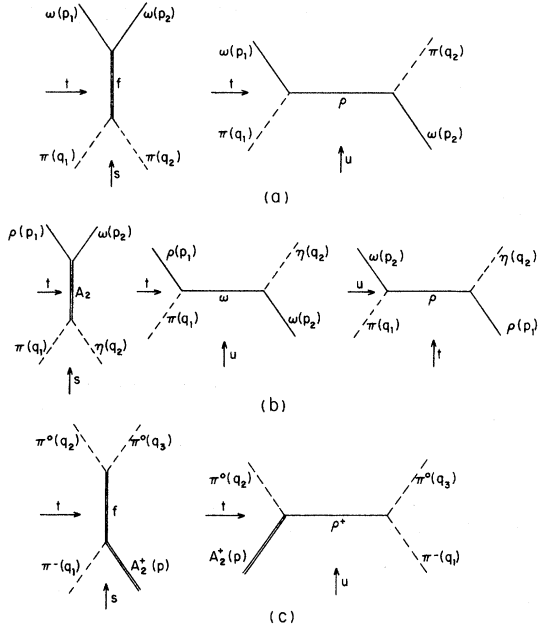


FIG. 1. The dual diagrams of the model for $V + P \rightarrow V' + P'$ [(a), (b)] and $P + T \rightarrow P' + P''$ [(c)] scattering. The dominating trajectories are specified.

A. The $P + V \rightarrow P + V$ process and the TVV couplings

Let us consider the scattering of pseudoscalar mesons (P) on vector mesons (V). If the amplitude

$$\mathcal{L}_{TVV} = \frac{g_{TV_1V_2}}{\mu} \tau^{\mu\nu} [\alpha \epsilon_\mu^{(1)} \epsilon_\nu^{(2)} + \beta_1 (\epsilon^{(1)} \cdot p_2) \epsilon_\mu^{(2)} p_{1\nu} + \beta_2 (\epsilon^{(2)} \cdot p_1) \epsilon_\mu^{(1)} p_{2\nu} + \gamma (\epsilon^{(1)} \cdot \epsilon^{(2)}) p_{1\mu} p_{2\nu} + \delta (\epsilon^{(1)} \cdot p_2) (\epsilon^{(2)} \cdot p_1) p_{1\mu} p_{2\nu}], \quad (1)$$

where $\epsilon^{(1)}(p_1)$, $\epsilon^{(2)}(p_2)$ are the polarization vectors of the vector mesons with four-momenta p_1 , p_2 , respectively, $\tau^{\mu\nu}$ is the polarization tensor of the tensor particle, μ is the pion mass, and $g_{TV_1V_2}$, α , $g_{TV_1V_2}\beta_1$, $g_{TV_1V_2}\beta_2$, $g_{TV_1V_2}\gamma$, and $g_{TV_1V_2}\delta$ are the five independent couplings of the TV_1V_2 vertex. The number of independent couplings is reduced for particular cases. Thus, if $V_1 = V_2$ there are only four independent couplings, if $V_1 = \gamma$ there are three, and for $V_1 = V_2 = \gamma$ there are only 2 independent couplings, the latter two reductions being the result of imposing gauge invariance.

The general requirements imposed on the dual amplitude of Ref. 7 lead to the following relations⁹ between the couplings defined in Eq. (1) and those of the exchanged vector mesons¹⁰:

$$4g_{T\pi\pi} g_{TV_1V_2} = g_{V_1\pi\rho} g_{V_2\pi\rho}, \quad (2a)$$

$$\alpha = p_1 \cdot p_2, \quad (2b)$$

$$\beta_1 = -\left(1 + \frac{2p_1^2}{l^2}\right), \quad (2c)$$

has a dual character, there are usually relations between the couplings of the particles exchanged in the direct and crossed channels. For presenting our approach we first take pions and isoscalar vector mesons (V is then an eigenstate of the charge-conjugation operator with $C = -1$). The leading contribution to the scattering in the s channel ($V_1 + V_2 \rightarrow P_1 + P_2$) comes from scalar and tensor mesons, while in the crossed channels vector and axial-vector mesons can be exchanged. Amplitudes for this process, embodying the features of crossing symmetry and correct asymptotic behavior, have been constructed by several authors.⁵⁻⁸ The amplitudes constructed by the various authors differ substantially in some details, since each of these papers uses a different approach for the additional constraints to be imposed on the amplitude, mainly in the low-energy region. In the following, we adopt the amplitude constructed in Ref. 7. In addition to crossing symmetry and Regge asymptotic behavior in all channels, our amplitude⁷ has no ancestors or daughters, no parity doubling of the ρ trajectory, and becomes automatically gauge invariant in the limit $M_{V_i} \rightarrow 0$. The leading contributions are then those of the f -meson exchange in the s channel and of the ρ -meson exchange in the t and u channels [see Fig. 1(a)].

For the TV_1V_2 effective interaction we use the definition

$$\beta_2 = -\left(1 + \frac{2p_2^2}{l^2}\right), \quad (2d)$$

$$\gamma = 3, \quad (2e)$$

$$\delta = -\frac{4}{l^2} \quad (2f)$$

where l_μ is the four-momentum of the tensor meson. The definitions of the various meson couplings encountered throughout this article are listed in Appendix A (except for the TVV and the TTP couplings which are defined and calculated in this section). In the particular case $V_1 = V_2 = \omega$, the appropriate relations read

$$g_{f\pi\pi} g_{f\omega\omega} = \frac{g_{\omega\rho\pi}^2}{4}, \quad (3a)$$

$$\beta_1 = \beta_2 = -\left(1 + \frac{2m_\omega^2}{M_f^2}\right). \quad (3b)$$

The value deduced for $g_{f\omega\omega}$ from Eq. (3) was previously used⁹ to calculate the rate for the $f \rightarrow \omega + \gamma$ decay.¹⁰

In order to discuss the decays $A_2 \rightarrow \omega\pi\pi$ and $f \rightarrow 4\pi$ we need to know the $g_{A_2\rho\omega}$ and $g_{f\rho\rho}$ couplings. We base this, of course, on the assumption that the $\langle T|V_1V_2\rangle$ vertex is mainly responsible for these decays. While for $A_2 \rightarrow \omega\pi\pi$ this appears as a natural assumption in view of the fact that the two pions are constrained to a state of isotopic spin 1, for the $f \rightarrow 4\pi$ mode other vertices could be also of importance. We shall return to this point in Sec. III.

Let us therefore consider the processes $\omega\pi \rightarrow \rho\eta$ and $\rho\pi \rightarrow \rho\pi$, from which the $g_{A_2\rho\omega}$ and $g_{f\rho\rho}$ ought to be derived. For the first process, the construction of the amplitudes proceeds along the same lines as for the $\omega\pi$ -scattering amplitude,⁷ the difference arising from the nonidentity of ω - ρ and π - η . Dividing the amplitudes into their symmetric and antisymmetric parts, one observes that the symmetric ones are analogous to the ω - π amplitudes. The leading contributions are then due to the A_2 meson in the direct channel and the symmetric contribution of ω and ρ mesons in the crossed channels as depicted in Fig. 1(b). We wish to emphasize that the antisymmetric combination of ω and ρ as well as terms proportional to η - π mass difference do not contribute to the leading terms in s .

In obtaining the coupling-constant relations [Eq. (2)] we find that (2a) now takes the form

$$4g_{A_2\pi\pi}g_{A_2\omega\rho} = \frac{1}{2}(g_{\rho\rho\eta} + g_{\omega\omega\eta})g_{\omega\rho\pi}. \quad (4)$$

In principle, the method should be applicable to π - ρ scattering, in which case the f and ω would appear as the leading trajectories in the neutral case, and the relations (2b)-(2f) and

$$g_{f\pi\pi}g_{f\rho\rho} = \frac{(g_{\omega\rho\pi})^2}{4} \quad (5)$$

in place of (2a) would result. There is, however, an objection to be made here. The dual character of the amplitude in all channels, together with crossing symmetry, is unable¹¹ to prevent the appearance of exotic resonances in the isotopic spin $I=2$ channels; a satisfactory solution to this problem has not been found. Thus, Eq. (5) does not have the same dynamical foundation as Eq. (4). Nevertheless, we feel it is appropriate to use it, since it is confirmed by the complementary approach of symmetry relations. Using SU(3) symmetry for the TVV interaction and canonical mixing for the vector- and tensor-meson multiplets, one obtains

$$g_{A_2\omega\rho} = g_{f\rho\rho} = g_{f\omega\omega}. \quad (6)$$

The relation (6) would result in our dynamical approach from Eqs. (3a), (4), and (5) if we use the same symmetry assumptions for the VVP and TTP

couplings (e.g., $g_{\eta\omega\omega} = g_{\eta\rho\rho} = (1/\sqrt{3})g_{\pi\omega\rho}$ and $g_{A_2\eta\pi} = (1/\sqrt{3})g_{f\pi\pi}$).

Numerically, one obtains from (3a), (5), and (6) (see Appendix A for the values of the experimentally determined couplings)

$$|g_{A_2\rho\omega}| = 1.93. \quad (7)$$

Our result can be compared with Renner's,¹² who has calculated the TVV couplings from a model based on tensor-meson dominance for the energy-momentum tensor. His results in our notation of Eqs. (2), (6), and (7) read: $|g_{f\omega\omega}^R| = 2.47$, $\alpha^R = p_1 \cdot p_2$, $\beta_1^R = \beta_2^R = -1$, $\gamma^R = 1$, $\delta^R = 0$. Although the approaches are basically different, the values of the dominant couplings are very close in these two models.

B. The $P+T \rightarrow P+P$ process and the TTP couplings

In our previous work⁷ we did not address ourselves to the $T+P \rightarrow P+P$ process. Therefore, we shall present here a full derivation of a dual amplitude for it, following closely Veneziano's work¹³ on $\omega + \pi \rightarrow \pi + \pi$.

Let us consider the process $A_2^+ + \pi^- \rightarrow \pi^0 + \pi^0$ and let q_1, q_2, q_3 be the (incoming) four-momenta of the charged and neutral pions, respectively. We define

$$s = (q_2 + q_3)^2, \quad t = (q_1 + q_2)^2, \quad u = (q_1 + q_3)^2, \quad (8)$$

$$k_\mu = (q_2 + q_3)_\mu, \quad \Delta_\mu = (q_3 - q_2)_\mu.$$

The general form of the amplitude for this process is

$$T = \epsilon_{\alpha\beta\gamma\delta} q_1^\alpha q_2^\beta q_3^\gamma \tau^{\delta\sigma} [k_\sigma A(s, t) + \Delta_\sigma B(s, t)], \quad (9)$$

where $\tau^{\delta\sigma}$ is the polarization tensor of the A_2 meson and $A(s, t), B(s, t)$ are invariant amplitudes, the first of them being antisymmetric and the second symmetric under the exchange of the like pions. The trajectories dominating the asymptotic behavior of the amplitude are the f in the s channel and the ρ in the t and u channels [Fig. 1(c)].

For the TTP effective Lagrangian we take

$$\mathcal{L}_{T_1 T_2 P} = \frac{g_{T_1 T_2 P}}{\mu} \epsilon_{\alpha\beta\gamma\delta} \tau^{(1)\alpha\mu} \tau^{(2)\nu\beta} p^\gamma q^\delta \times \left(g_1 g_{\mu\nu} + \frac{g_2}{\mu^2} l_\mu l_\nu \right), \quad (10)$$

where $\tau^{(1)}(p), \tau^{(2)}(q)$ are the polarization tensors of the tensor mesons and l is the pseudoscalar-meson momentum.

A suitable dual representation for the amplitude (8) is then

$$A = g \frac{\alpha_t - \alpha_u}{2 - \alpha_t - \alpha_u} F(s, t, u), \quad (11a)$$

$$B = gF(s, t, u), \quad (11b)$$

where g is a constant and

$$F = -\frac{\epsilon'}{2} \left[\frac{\Gamma(1-\alpha_t)\Gamma(2-\alpha_s)}{\Gamma(3-\alpha_t-\alpha_s)} + \frac{\Gamma(1-\alpha_u)\Gamma(2-\alpha_s)}{\Gamma(3-\alpha_u-\alpha_s)} \right. \\ \left. + \frac{\Gamma(1-\alpha_t)\Gamma(1-\alpha_u)}{\Gamma(2-\alpha_t-\alpha_u)} \right]. \quad (12)$$

For the assumed degenerate vector-tensor trajectory we take a value representing an average of experimental fits,¹⁴ $\alpha_x = 0.46 + \epsilon'x$ and $\epsilon' = 0.9$ GeV^{-2} . Note that for the external masses involved in this process $\alpha_s + \alpha_t + \alpha_u = 3$.

The requirement that the amplitudes (11) have the correct residues at the f and ρ poles reads as follows:

$$\text{Res}_{s=m_f^2} A = g(\alpha_t - \alpha_u) = \frac{g_{f\pi\pi} g_{A_2 f\pi} g_2}{\mu^4} (t-u), \quad (13a)$$

$$\text{Res}_{t=m_\rho^2} A = g = \frac{g_{A_2 \rho\pi} g_{\rho\pi\pi}}{\mu^2}, \quad (13b)$$

$$\text{Res}_{s=m_f^2} B = g = -\frac{2g_{A_2 f\pi} g_1 g_{f\pi\pi}}{\mu^2}, \quad (13c)$$

$$\text{Res}_{t=m_\rho^2} B = g = \frac{g_{A_2 \rho\pi} g_{\rho\pi\pi}}{\mu^2}. \quad (13d)$$

Equations (13) give for the two independent TTP couplings

$$g_{A_2 f\pi} = -\frac{g_{A_2 \rho\pi} g_{\rho\pi\pi}}{2g_{f\pi\pi}}, \quad (14a)$$

$$g_1 = -\frac{g_2}{2\epsilon'\mu^2} = 1. \quad (14b)$$

Numerically, using the experimentally determined values for the couplings in the right-hand side of (14a) one has

$$|g_{A_2 f\pi}| = 1.80. \quad (15)$$

There is only one previous determination of a TTP coupling in the literature. By using current-algebra sum rules, Gilman and Harari¹⁵ arrived at $|g_{A_2 f\pi}| = 2.8$, which is fairly close to our value (15) [in their expression for the TTP vertex the second term in Eq. (10) is ignored].

III. THE STRONG DECAYS $T \rightarrow V + 2P$

We proceed now to calculate the rates for the partial decay modes $A_2 \rightarrow \omega\pi\pi$ and $f \rightarrow \rho\pi\pi$. To this end, we picture the amplitude $T+P \rightarrow V+P$ as

$$F_{(t+u)} = -\frac{\epsilon'}{2} \left[\frac{\Gamma(1-\alpha_t)\Gamma(3-\alpha_s)}{\Gamma(4-\alpha_t-\alpha_s)} + \frac{\Gamma(1-\alpha_u)\Gamma(3-\alpha_s)}{\Gamma(4-\alpha_u-\alpha_s)} + \frac{\Gamma(1-\alpha_u)\Gamma(1-\alpha_t)}{\Gamma(2-\alpha_u-\alpha_t)} + \dots \right], \quad (17)$$

$$F_{(s)} = -\frac{\epsilon'}{2} \left[\frac{\Gamma(3-\alpha_t)\Gamma(1-\alpha_s)}{\Gamma(4-\alpha_t-\alpha_s)} + \frac{\Gamma(3-\alpha_u)\Gamma(1-\alpha_s)}{\Gamma(4-\alpha_u-\alpha_s)} + \frac{\Gamma(3-\alpha_u)\Gamma(3-\alpha_t)}{\Gamma(6-\alpha_t-\alpha_u)} + \dots \right], \quad (18)$$

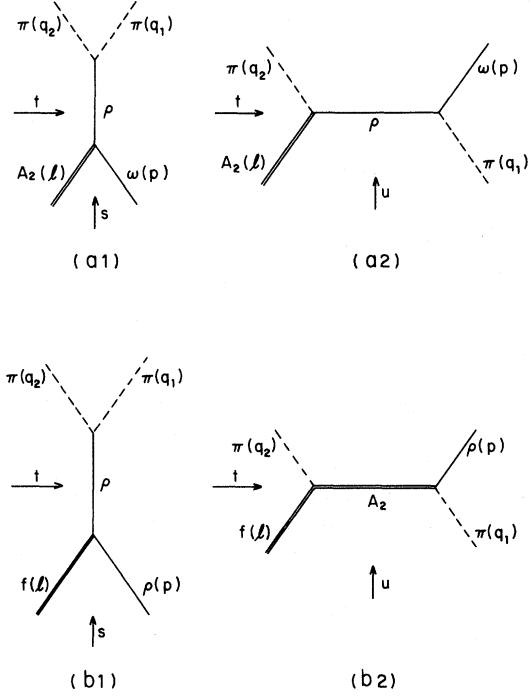


FIG. 2. The contributions included in the present model for the decays $A_2 \rightarrow \omega\pi\pi$ [(a)] and $f \rightarrow \rho\pi\pi$ [(b)].

receiving contributions from resonances in the direct channel and Regge-trajectory exchanges in the crossed channels. The relevant contributions for these decays and the definition of the three channels are depicted in Fig. 2. To combine both these contributions we use the same dual mechanism as described in Sec. II for $V-P$ scattering⁷ and for $T+P \rightarrow P+P$.

The general form of the $T+P \rightarrow V+P$ amplitude is expressed in terms of eight independent amplitudes. Details concerning these amplitudes are relegated to Appendix B. Here we want to emphasize that in the present model these amplitudes are decomposed into two parts of the general form

$$A_i = R_i^{(t+u)} F_{(t+u)}(s, t) + R_i^{(s)} F_{(s)}(s, t), \quad (16)$$

where $R_i^{(t+u)}$ contain the residue of the $\rho(A_2)$ exchange in the t and u channels of $A_2 + \pi \rightarrow \omega + \pi$ ($f + \pi \rightarrow \rho + \pi$), and $R_i^{(s)}$ contain the residue of ρ in the s channels of both reactions. For the $A_2 + \pi \rightarrow \omega + \pi$ reaction, $F_{(t+u)}$ and $F_{(s)}$ are given by

TABLE I. The calculated partial widths in MeV for the $A_2 \rightarrow \omega\pi\pi$ and $f \rightarrow \rho\pi\pi$ decays. The meaning of the various columns is explained in the text.

	Γ_{Born}^s	Γ_{dual}^s	$\Gamma_{\text{Born}}^{t+u}$	$\Gamma_{\text{dual}}^{t+u}$	$\Gamma_{(-)}^{\text{theor}}$	$\Gamma_{(+)}^{\text{theor}}$
$A_2 \rightarrow \omega\pi^+\pi^-$	0.92	0.975	0.054	0.27	0.30	2.2
$f \rightarrow \rho^0\pi^+\pi^-$	0.53	0.44	0.67×10^{-2}	0.9×10^{-2}	0.40	0.49

where ϵ' is the slope of the ρ - A_2 Regge trajectory. The asymptotic behavior of these expressions is

$$F_{(t+u)} \xrightarrow{s \rightarrow \infty} -\frac{\epsilon'}{2} \Gamma(1 - \alpha_t) (1 - e^{-i\pi\alpha_t}) \left(\frac{s}{s_0}\right)^{\alpha_t - 1}, \quad (19a)$$

$$F_{(t+u)} \xrightarrow{t \rightarrow \infty} -\frac{\epsilon'}{2} \Gamma(3 - \alpha_s) (1 - e^{-i\pi\alpha_s}) \left(\frac{t}{t_0}\right)^{\alpha_s - 3}, \quad (19b)$$

$$F_{(s)} \xrightarrow{s \rightarrow \infty} -\frac{\epsilon'}{2} \Gamma(3 - \alpha_t) (1 - e^{-i\pi\alpha_t}) \left(\frac{s}{s_0}\right)^{\alpha_t - 3}, \quad (19c)$$

$$F_{(s)} \xrightarrow{t \rightarrow \infty} -\frac{\epsilon'}{2} \Gamma(1 - \alpha_s) (1 - e^{-i\pi\alpha_s}) \left(\frac{t}{t_0}\right)^{\alpha_s - 1}. \quad (19d)$$

From (16) and (19) one sees that for this process there is a decoupling of the leading- s behavior from the leading- t behavior and therefore one cannot produce a relation between the couplings entering $R^{(t+u)}$ and $R^{(s)}$, as it was the case⁷ for the process $V + \pi \rightarrow V + \pi$. Similar amplitudes and conclusions hold for the $f + \pi \rightarrow \rho + \pi$. If such a relation would have been possible, one would have an additional way to calculate the $A_2\rho\omega$ vertex, this time in terms of $A_2\rho\pi$, $\rho\omega\pi$, and $\rho\pi\pi$ couplings. More important, the phase between the contributions of the various channels would have been thus determined.

The reason for this decoupling can be traced to the fact that owing to the higher spin of the participating particles, there are now more invariant (and helicity) amplitudes demanding stronger constraints on their asymptotic behavior than in $V-\pi$ scattering. These constraints fix the asymptotic behavior of certain combinations of the invariant amplitudes down to order $s^{\alpha_t - 2}$. The terms describing the ρ exchange in the s channel do not fulfill the abovementioned asymptotic constraints, their highest order going only as $s^{\alpha_t - 3}$.

The decay rate $T \rightarrow V\pi\pi$ is given by

$$\Gamma(T \rightarrow V\pi\pi) = \frac{1}{(2\pi)^3} \frac{1}{2^5(5)M_T^3} \times \int_{4\mu^2}^{(M-m)^2} ds \int_{-2kq}^{2kq} \sum |M|^2 dt, \quad (20)$$

where $\sum |M|^2$ is the summation over the helicity amplitudes, M_T is the mass of the decaying particle, m is the vector-meson mass, and

$$k = \frac{\{[s - (M_T - m)^2][s - (M_T + m)^2]\}^{1/2}}{2\sqrt{s}} \quad (21)$$

$$q = \frac{(s - 4\mu^2)^{1/2}}{2}.$$

We calculate the rate given by the contributions depicted in Fig. 2 by using their analytic expressions, as given in Appendix B for $A_2 \rightarrow \omega\pi\pi$; similar expressions, not listed for reasons of economy, hold for $f \rightarrow \rho\pi\pi$ (the main difference is in the t and u -channel exchanges, which are of tensor type in the latter). In Appendix A are listed numerical values of the coupling constants we use; the majority of them are experimentally determined, while for the TVV and TTP couplings we use the values derived from our model [Eqs. (2), (7), and (15)].

In order to get a feeling for the relative importance of the various contributions, as well as for the modifications of the dual model relative to the Born model, we present them as separate entities in Table I. $\Gamma_{\text{Born}}^s, \Gamma_{\text{dual}}^s$ are the widths obtained if only the s -channel contribution is taken, using either the Born term or the corresponding one given by the dual model. $\Gamma_{\text{Born}}^{t+u}, \Gamma_{\text{dual}}^{t+u}$ are similarly defined. $\Gamma_{(-)}^{\text{theor}}, \Gamma_{(+)}^{\text{theor}}$ are the predictions of our model containing both s and $t+u$ exchange, for the two possible relative phases. Needless to say, in light of the experimental findings^{3,4} we favor the constructive-interference results of our model,

$$\Gamma^{\text{theor}}(A_2^0 \rightarrow \omega\pi^+\pi^-) = 2.2 \text{ MeV},$$

$$\Gamma^{\text{theor}}(f^0 \rightarrow \rho^0\pi^+\pi^-) = 0.49 \text{ MeV}.$$

This is to be compared with the experimental average¹⁶ of

$$\Gamma^{\text{exp}}(A_2 \rightarrow \omega\pi\pi) = 8.6 \pm 1.8 \text{ MeV},$$

$$\Gamma^{\text{exp}}(f^0 \rightarrow \pi^+\pi^-\pi^+\pi^-) = 6.2 \pm 1.5 \text{ MeV}.$$

As can be seen from Table I, the main contribution to the decays is due, in our model, to the chain $T \rightarrow (V') + V \rightarrow \pi + \pi + V$. The dual representation for this term affects only slightly its Born approximation value. We note also that the factor of 1.8 between the values of Γ_{Born}^s for A_2 and f decays is due to phase space and the kinematic dependence of α . The contributions from the crossed chan-

nels [diagrams (a2) and (b2) in Fig. 2] are smaller in the Born approximation by at least an order of magnitude vis-à-vis the direct-channel contributions.¹⁷ The dual representation enhances these terms, the effect being particularly large for $A_2 \rightarrow \omega\pi\pi$. Here, the positive interference of Γ_{dual}^s and $\Gamma_{\text{dual}}^{t+u}$ leads to a value which is twice as large as the direct-channel contribution taken alone. Even so, our prediction (the last column of Table I) is 4 times smaller than the average experimental value. A comparison of our result for $f \rightarrow \rho\pi\pi$ with experiment is less transparent since the experimental analyses of $f \rightarrow 4\pi$ did not separate the $\rho\pi\pi$ subset unambiguously. An examination of the published data⁴ indicates that it could account at most for 50% of the $f \rightarrow 4\pi$ decay. Thus, here again our prediction is smaller than the average experimental value, by a factor of ~ 6 . We checked also the magnitude of the contribution of possible pion exchange [$f \rightarrow (\pi)\pi \rightarrow \rho\pi\pi$] and we found it to be only about $\frac{1}{3}$ of the A_2 -exchange Born term.

Previous approaches to these decays have considered the exchange of axial-vector mesons as the primary mechanism. The relevant $fA_1\pi$ coupling entering the $f \rightarrow 4\pi$ calculation has been obtained by Parashar¹⁸ from a quark model, while Bányai and Rittenberg¹⁹ have used a chiral-symmetric Lagrangian in their treatment. Golowich²⁰ has considered the $A_2 \rightarrow \omega\pi\pi$ mode as proceeding through B -meson exchange. In order to account¹⁸⁻²⁰ for the observed rates, unreasonably large (in our opinion) coupling constants are required, e.g., $g_{BA_2\pi^2}/4\pi \simeq 70$.

It is therefore of interest to be able to distinguish experimentally between the two mechanisms. We have calculated the distributions $d\sigma/dM(VP)$ and $d\sigma/dm^2(PP)$ for both decays in our dual model and in a model with axial-vector-meson exchanges only. In Fig. 3 we give the distribution for $A_2 \rightarrow \omega\pi\pi$. The $\omega\pi$ effective-mass plot includes the histogram obtained by Diaz *et al.*^{3(c)} It seems very unlikely from it that B exchange contributes significantly to this decay mode. The fit given by our model is gratifying, and we remark that the excess of events with high effective $\omega\pi$ mass can probably be accounted for by including the width of A_2 in the model calculation. There are no experimental histograms for the $\pi\pi$ effective mass to compare with.

In Fig. 4 we give the theoretical curves obtained with the two approaches for $f \rightarrow \rho\pi\pi$ without comparing with experimental data, since, as noted before, the $\rho\pi\pi$ subset has not been extracted. However, the experimental data for $f \rightarrow 4\pi$ have been compared by Anderson *et al.*^{4(c)} with the $\rho\rho$ model of Ascoli *et al.*^{4(a)} and with the calculation of Bányai and Rittenberg,¹⁹ clearly favoring

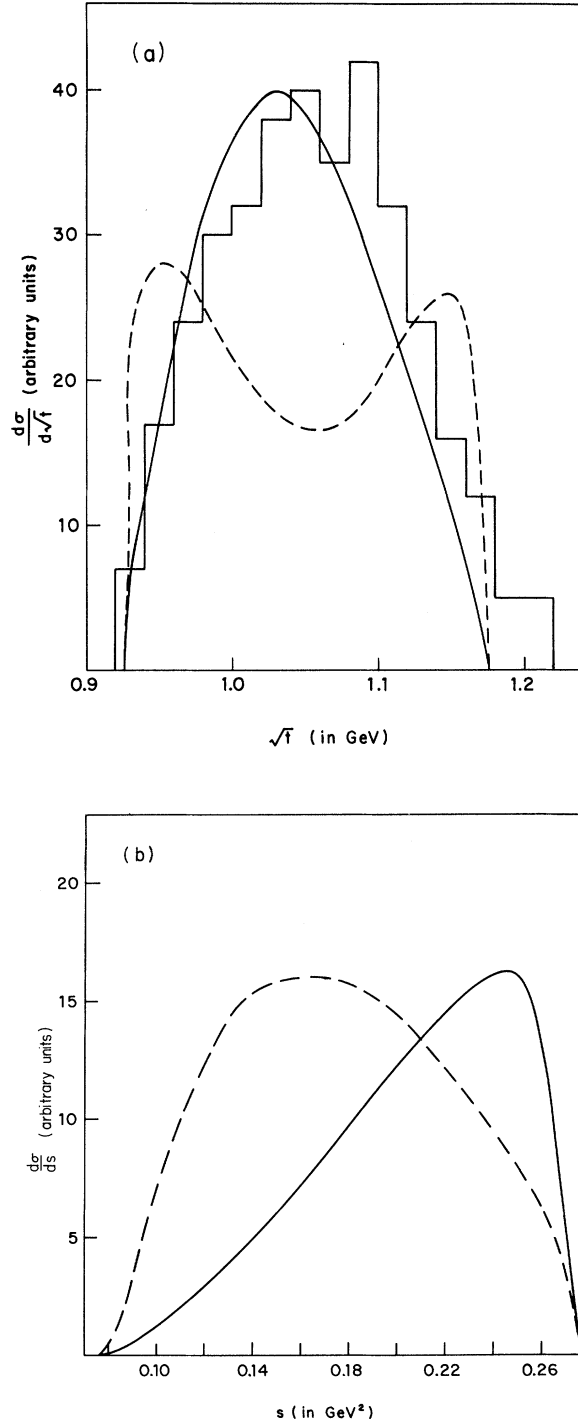


FIG. 3. Effective-mass distributions for the decay $A_2 \rightarrow \omega\pi\pi$. (a) $d\sigma/d\sqrt{t}$, where $t = (p_\omega + p_\pi)^2$; (b) $d\sigma/ds$, where $s = (p_\pi^{(1)} + p_\pi^{(2)})^2$. The solid line is calculated with our model and the dashed curve is the result of a model involving axial-vector-meson exchange. The experimental data are from Ref. 3(c). The theoretical curves of (a) are the best χ^2 normalization of the respective model to the data.

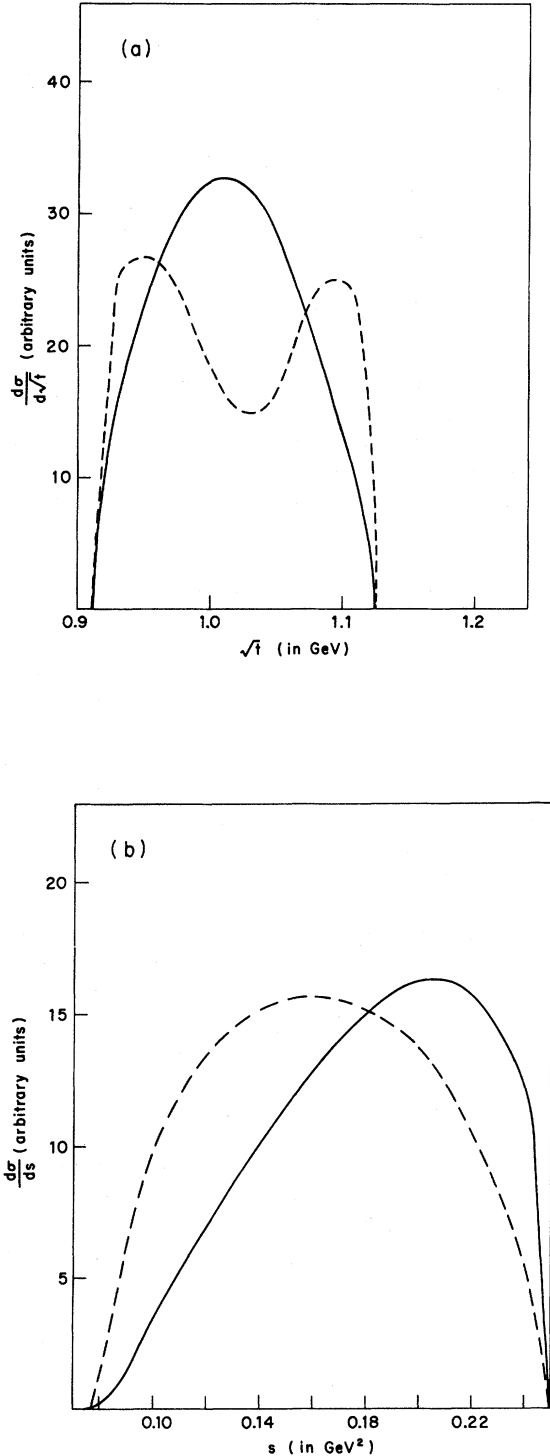


FIG. 4. Effective-mass distributions for the decay $f \rightarrow \rho\pi\pi$. (a) $d\sigma/d\sqrt{t}$, where $t = (p_\rho + p_\pi)^2$; (b) $d\sigma/ds$, where $s = (p_\pi^{(1)} + p_\pi^{(2)})^2$. The solid curve is calculated with our model and the dashed curve is the result of a model involving axial-vector-meson exchange.

the $\rho\rho$ model.

From the SU(6)-symmetry structure of the vertices entering in the dual amplitude for $T + \pi \rightarrow V + \pi$, we expect also the decay $K^{**} \rightarrow K^*\pi\pi$ to occur. In this case, however, the pions are allowed to be in both $I=0$ and 1 states; our model accounts only for the $I=1$ channel. The dominant contributions in our model are ρ exchange in the s channel and K^* exchange in the crossed channels. Using the symmetry values $g_{K^{**}K^*\rho} = \frac{1}{2}g_{A_2\omega\rho}$, $g_{K^{**}K^*\pi} = (1/\sqrt{2})g_{\omega\rho\pi}$, and the experimental $g_{K^{**}K^*\pi}$, we get 0.46 MeV for the mode $K^{**} \rightarrow K^*\pi^+\pi^-$ and twice as much for the $K^{**} \rightarrow K^*\pi^+\pi^0$ one.

IV. ELECTROMAGNETIC DECAYS

Although the electromagnetic decays of tensor mesons have yet to be detected, there are already several theoretical calculations^{9,12,21-27} with quite divergent predictions for their expected rates. The models on which these calculations are based range from the tensor-meson dominance of the energy-momentum tensor^{12,23} through finite-energy sum rules^{21,22} and the dispersion-relations approach^{24,25} to quark²⁶ and symmetry models.²⁷

The dual amplitude for the $P + V \rightarrow P' + V'$ process⁷ was constructed so that it becomes gauge invariant in the limit $m_V \rightarrow 0$ or both $m_V \rightarrow 0$, $m_{V'} \rightarrow 0$, the amplitude thus being suitable for describing processes like $V + P \rightarrow \gamma + P'$ and $\gamma + P \rightarrow \gamma + P'$. Applying⁹ the procedure described in Sec. II, we derive now the electromagnetic couplings of $TV\gamma$ and $T\gamma\gamma$ types which read as follows:

$$g_{f\omega\gamma} = \frac{g_{\omega\rho\pi}g_{\rho\pi\gamma}}{4g_{f\pi\pi}}, \quad g_{f\rho\gamma} = \frac{g_{\omega\rho\pi}g_{\omega\pi\gamma}}{4g_{f\pi\pi}}, \quad (22)$$

$$g_{f\gamma\gamma} = \frac{g_{\omega\pi\gamma}^2 + g_{\rho\pi\gamma}^2}{4g_{f\pi\pi}};$$

$$g_{A_2\omega\gamma} = \frac{g_{\omega\omega\pi}g_{\omega\pi\gamma} + g_{\rho\pi\gamma}g_{\omega\rho\pi}}{8g_{A_2\pi\pi}},$$

$$g_{A_2\rho\gamma} = \frac{g_{\rho\rho\pi}g_{\rho\pi\gamma} + g_{\omega\pi\gamma}g_{\omega\rho\pi}}{8g_{A_2\pi\pi}}, \quad (23)$$

$$g_{A_2\gamma\gamma} = \frac{g_{\rho\pi\gamma}g_{\rho\pi\gamma} + g_{\omega\pi\gamma}g_{\omega\pi\gamma}}{4g_{A_2\pi\pi}}.$$

The values of the $\alpha, \beta_1, \beta_2, \gamma, \delta$ couplings are as given in Eq. (2). Note that if the $VVP, \gamma VP,$ and TPP couplings are related by nonet-symmetry relations, the tensor couplings arrived at in (22) and (23) obey it as well, namely

$$g_{f\omega\gamma} = \frac{1}{3}g_{f\rho\gamma} = g_{A_2\rho\gamma} = \frac{1}{3}g_{A_2\omega\gamma} \quad (24)$$

$$g_{A_2\gamma\gamma} = \frac{3}{5}g_{f\gamma\gamma}. \quad (25)$$

Using experimentally determined values (Appendix A) we calculate $g_{f\rho\gamma}$ in (22) to be

$$g_{f\rho\gamma} = 9.65 \times 10^{-2}. \quad (26)$$

The numerical value of $g_{f\gamma\gamma}$ is similarly obtained, taking now for $g_{\rho\pi\gamma}$ the SU(6) value ($= \frac{1}{3}g_{\omega\pi\gamma}$)

$$g_{f\gamma\gamma} = 5.38 \times 10^{-3}. \quad (27)$$

For the remaining electromagnetic couplings of Eqs. (22) and (23) we use the symmetry values given in Eqs. (24) and (25).

$$|M_{T \rightarrow \gamma + V_2}|^2 = \frac{g_{TVV_2}^2}{\mu^2} \left\{ 3\alpha^2 + \frac{k^2}{m^2} \left[\alpha + \frac{1}{2}\beta_2(M_T + m)^2 \right] \left[\alpha + \frac{1}{2}\beta_2(M_T - m)^2 \right] + \frac{1}{3}(2\gamma k^2 - \alpha)^2 \right\}, \quad (28)$$

with $k^2 = (M_T^2 - m^2)^2 / 4M_T^2$, m being the vector-meson mass. For $T \rightarrow \gamma + \gamma$, $|M|^2$ is given by

$$|M_{T \rightarrow \gamma\gamma}|^2 = \frac{g_{T\gamma\gamma}^2}{\mu^2} \left[2\alpha^2 + \frac{1}{3} \left(\alpha - \gamma \frac{M_T^2}{2} \right)^2 \right]. \quad (30)$$

Inserting the particular values of our model for α , β_2 , and γ given in Eq. (2) into (29), (30), and (28) one has

$$\Gamma_{T \rightarrow V\gamma} = \frac{g_{TVV}^2}{4\pi} \frac{M_T^3}{80\mu^2} (1-x)^3 \left[\frac{10}{3} - 4x + 3x^2 + x^3 \right], \quad (31)$$

$$x = \left(\frac{m}{M_T} \right)^2,$$

$$\Gamma_{T \rightarrow \gamma\gamma} = \frac{g_{T\gamma\gamma}^2}{4\pi} \frac{M_T^3}{48\mu^2}. \quad (32)$$

We present in Table II, column 2, the predictions of our model for the decay widths of one- and two-photon decay modes of f and A_2 , the results of other models being also tabulated for comparison.²⁸ No experimental data are available so far.

V. SUMMARY

We have presented in this paper a calculation of tensor-meson decays $T \rightarrow V + 2P$, $T \rightarrow V + \gamma$, $T \rightarrow 2\gamma$. The correlating factor for all these decays is the TVV coupling, which we have set out to calculate with the aid of a dual model for $P + V \rightarrow P' + V'$ amplitudes. Our results for the strong couplings are given in Eqs. (2), (3), (6), and (7), and those for

The width for a decay $T \rightarrow V_1 + V_2$ is given by

$$\Gamma(T \rightarrow V_1 + V_2) = \frac{k|M|^2}{40\pi M_T^2}, \quad (28)$$

where $|M|^2$ is the square of the amplitude for decay summed over polarizations. Using the general vertex defined in Eq. (1), with $\epsilon^{(1)}$ the polarization vector of the photon, $|M|^2$ takes the form

the electromagnetic ones are given in Eqs. (22)–(27) and (2).

The calculation of $A_2 \rightarrow \omega\pi\pi$ and $f \rightarrow \rho\pi\pi$ was performed by building an appropriate $T + P \rightarrow V + P$ dual amplitude and has also necessitated the determination of the TTP coupling [Eqs. (14) and (15)]. Our results for these rates turn out to be, by a factor of ~ 4 , smaller than the average experimental values. This raises the question of whether the TVV vertex is indeed the dominant one. A comparison with other models, especially those including axial-vector-meson exchanges, was presented in Sec. III and in view of the very large couplings required by these models we doubt that they constitute the major contribution. On the other hand, it might well be that our theoretical relations for the g_{TVV} couplings are realized only within factors of ~ 2 . If instead of (7) one has $|g_{A_2\rho\omega}| \simeq 4$, the proposed mechanism can account well for the $T \rightarrow VPP$ decays, while the dimensionless couplings are still of very reasonable magnitude ($g_{A_2\rho\omega}^2/4\pi \simeq 1.3$). Measurements of the various distributions suggested would help to answer this question. The results in Fig. 3 are very encouraging for the TVV approach.

In this connection one should also upgrade our estimate in Sec. III for the $K^{**} \rightarrow K^*(\pi\pi)_{I=1}$ by a factor of ~ 4 . Thus, keeping in mind that there could also be some contribution from the $(\pi\pi)_{I=0}$ state, we expect $K^{**} \rightarrow K^*\pi\pi$ to be at least 5.5 MeV. We remark that so far the detection of this

TABLE II. The calculated partial decay widths for one- and two-photon decays of f and A_2 .

Decay mode	Present calculation	Ref. 12	Ref. 21	Ref. 22	Ref. 23	Ref. 24	Ref. 26	Ref. 27
$f \rightarrow \omega\gamma$ (MeV)	0.060	0.2	0.096 or 0.24	...
$f \rightarrow \rho\gamma$ (MeV)	0.58	2.0	1.3	...	0.84 or 2.2	...
$A_2 \rightarrow \omega\gamma$ (MeV)	0.68	0.84 or 2.5	...
$A_2 \rightarrow \rho\gamma$ (MeV)	0.080	0.11 or 0.29	...
$f \rightarrow \gamma\gamma$ (keV)	5.07	8.0	0.8	5.7	7	11.3	1.2 or 2.3	1
$A_2 \rightarrow \gamma\gamma$ (keV)	2.05	...	0.3	0.46 or 0.81	...

mode has not been reported.¹⁶

Before concluding, we should like to emphasize that the experimental data we are referring to in our comparisons are averages¹⁶ over widely spread experimental results, some of which^{3(c),3(d)} go as high as $\Gamma(A_2^0 \rightarrow \omega^0 \pi^+ \pi^-) \sim 20$ MeV. If these turn out to be correct, our picture for the decays would imply a rate for $K^{**} \rightarrow K^* \pi \pi$ of at least 13 MeV, while the electromagnetic decays listed in Table II would also then be higher by a factor of ~ 20 . This would mean that modes like $f \rightarrow \rho \gamma$, $A_2 \rightarrow \omega \gamma$ would have widths of about 10 MeV, if indeed the relation between the strong and the electromagnetic decay mechanisms is as pictured here. The magnitude of the TVV couplings affects also the rate of hadron production in the $\gamma\gamma$ events of $e^+e^- \rightarrow e^+e^- +$ hadrons, being of particular interest if these events are dominated by resonances.^{22,27} An experimental effort to measure the strength of the electromagnetic vertices of tensor mesons in decays and colliding beam experiments, and to improve the data on $T \rightarrow V + 2\pi$ decays, is of time-ly interest.

APPENDIX A

The following definitions for vertices, and values for the coupling constants determined from measured widths are used in the text. Generally, we shall use the notation $M(p) \rightarrow m_1(q_1) + m_2(q_2)$, the mass μ denoting pion mass;

$$q = \frac{1}{2M} [M^2 - (m_1 + m_2)^2]^{1/2} [M^2 - (m_1 - m_2)^2]^{1/2},$$

$$\Delta_\mu = (q_1 - q_2)_\mu.$$

$\rho\pi\pi$ vertex. $g_{\rho\pi\pi} \epsilon_{(\rho)}^\mu \Delta_\mu$:

$$\Gamma(\rho \rightarrow \pi\pi) = \frac{g_{\rho\pi\pi}^2}{4\pi} \frac{2}{3} \frac{q^3}{m_\rho^2},$$

$$\Gamma^{\text{exp}}(\rho \rightarrow \pi\pi) = 146 \text{ MeV}, \quad g_{\rho\pi\pi} = 5.93.$$

$f\pi\pi$ vertex. $(g_{f\pi\pi}/\mu) \tau^{\mu\nu} \Delta_\mu \Delta_\nu$:

$$\Gamma(f \rightarrow \pi\pi) = \frac{g_{f\pi\pi}^2}{4\pi} \frac{8}{5} \frac{q^5}{\mu^2 M^2},$$

$$\Gamma^{\text{exp}}(f \rightarrow \pi\pi) = 141 \text{ MeV}, \quad g_{f\pi\pi} = 0.613.$$

PV_1V_2 vertex. $(g_{PV_1V_2}/\mu) \epsilon_{\alpha\beta\gamma\delta} \epsilon_1^\alpha q_1^\beta \epsilon_2^\gamma q_2^\delta$:
For $\omega\rho\pi$, assuming $\omega \rightarrow (\rho\pi) \rightarrow 3\pi$,

$$\Gamma(\omega \rightarrow 3\pi) = \frac{g_{\omega\rho\pi}^2}{4\pi} \frac{g_{\rho\pi\pi}^2}{4\pi} \times 8.55 \text{ MeV},$$

$$\Gamma^{\text{exp}}(\omega \rightarrow 3\pi) = 9 \text{ MeV}, \quad g_{\omega\rho\pi} = 2.17.$$

For $\omega\pi\gamma$,

$$\Gamma(\omega \rightarrow \pi\gamma) = \frac{g_{\omega\pi\gamma}^2}{4\pi} \frac{q^3}{3\mu^2},$$

$$\Gamma^{\text{exp}}(\omega \rightarrow \pi\gamma) = 0.87 \text{ MeV}, \quad g_{\omega\pi\gamma} = 0.109.$$

TVP vertex. $(g_{TVP}/\mu^2) \epsilon_{\alpha\beta\gamma\delta} \tau^{\alpha\mu} q_{2\mu} q_1^\beta p^\gamma \epsilon_{(\nu)}^\delta$:

$$\Gamma(T \rightarrow V\pi) = \frac{g_{TVP}^2}{4\pi} \frac{q^5}{5\mu^4};$$

for $A_2\rho\pi$,

$$\Gamma^{\text{exp}}(A_2 \rightarrow \rho\pi) = 71 \text{ MeV}, \quad g_{A_2\rho\pi} = 0.373;$$

and for $K^{**}K^*\pi$,

$$\Gamma^{\text{exp}}(K^{**} \rightarrow K^*\pi) = 29.5 \text{ MeV}, \quad g_{K^{**}K^*\pi} = 0.237.$$

The experiment agrees well with the SU(6) relation $g_{K^{**}K^*\pi} = (\sqrt{3}/2\sqrt{2})g_{A_2\rho\pi}$.

APPENDIX B

This appendix contains the definition of the invariant amplitudes and, following that, the helicity amplitudes for the process $T(l) + V(p) \rightarrow \pi(q_1) + \pi(q_2)$. At last we give the invariant amplitudes for the decay $A_2 \rightarrow \omega\pi\pi$, first in the Born approximation: the ρ exchange in the $t+u$ channels ($A_{i,\text{Born}}^{t+u}$) and the ρ exchange in the s channel ($A_{i,\text{Born}}^s$). The dual representation for the invariant amplitudes is then given in terms of $R_i^{(t+u)}$ and $R_i^{(s)}$ (their definition is given in the text (Sec. III); the s, t, u channels are depicted in Fig. 2).

The eight invariant amplitudes are defined by

$$\begin{aligned} T_{\alpha\beta\gamma} = & A_1 g_{\alpha\gamma} k_\beta + A_2 g_{\alpha\gamma} \Delta_\beta + (A_3 k_\gamma + A_6 \Delta_\gamma) k_\alpha k_\beta \\ & + (A_4 k_\gamma + A_7 \Delta_\gamma) k_\alpha \Delta_\beta + (A_5 k_\gamma + A_8 \Delta_\gamma) \Delta_\alpha \Delta_\beta, \end{aligned} \quad (\text{B1})$$

with

$$k_\mu = (q_1 + q_2)_\mu, \quad \Delta_\mu = (q_1 - q_2)_\mu.$$

The two pions are in a state of isotopic spin $I=1$, hence under the exchange of q_1 and q_2 or $t \leftrightarrow u$ the invariant amplitudes obey the following symmetry relations:

$$A_{2i}(t, u) = A_{2i}(u, t) \quad (\text{B2})$$

$$A_{2i-1}(t, u) = -A_{2i-1}(u, t),$$

$i=1, \dots, 4$. The helicity amplitudes are defined by

$$M_{\lambda\mu} = \tau_{(\lambda)}^{\alpha\beta} \epsilon_{(\mu)}^\gamma T_{\alpha\beta\gamma} \quad (\text{B3})$$

$$\lambda = 2, \dots, -2, \quad \mu = 1, 0, -1$$

and their explicit expressions in the s channel are

$$\begin{aligned}
M_{2,1} &= (\sqrt{2}q \sin\theta)[A_2 - (\sqrt{2}q \sin\theta)^2 A_8], \\
M_{2,0} &= \frac{(\sqrt{2}q \sin\theta)^2}{m} (\sqrt{s} p A_5 + 2p_0 q \cos\theta A_8), \\
M_{2,-1} &= (\sqrt{2}q \sin\theta)^3 A_8, \\
M_{1,1} &= \frac{1}{\sqrt{2}M_T} [(\sqrt{2}q \sin\theta)^2 (4l_0 q \cos\theta A_8 - \sqrt{s} p A_7) + A_1 \sqrt{s} p - 2q l_0 \cos\theta A_2], \\
M_{1,0} &= \frac{q \sin\theta}{m M_T} [2q p_0 \cos\theta (\sqrt{s} p A_7 - 4l_0 q \cos\theta A_8) + \sqrt{s} p (\sqrt{s} p A_4 - 4l_0 q \cos\theta A_5) + A_2 l \cdot p], \\
M_{1,-1} &= \frac{\sqrt{2}q^2 \sin^2\theta}{M_T} (\sqrt{s} p A_7 - 4l_0 q \cos\theta A_8), \\
M_{0,1} &= -\frac{2q \sin\theta}{\sqrt{3}} \left\{ \left(\frac{\sqrt{s} p}{M_T} \right)^2 A_6 - \frac{\sqrt{s} p}{M_T^2} 2l_0 \cos\theta A_7 + \left[\left(\frac{2q l_0 \cos\theta}{M_T} \right)^2 - (\sqrt{2}q \sin\theta)^2 \right] A_8 + \frac{1}{2} A_2 \right\}, \\
M_{0,0} &= \frac{\sqrt{2}}{\sqrt{3}m} \left\{ \left(\frac{\sqrt{s} p}{M_T} \right)^2 (\sqrt{s} p A_3 + 2p_0 q \cos\theta A_6) - \frac{2l_0 \sqrt{s} q p \cos\theta}{M_T^2} (\sqrt{s} p A_4 + 2p_0 q \cos\theta A_7) \right. \\
&\quad \left. + \left[\left(\frac{2q l_0 \cos\theta}{M_T} \right)^2 - (\sqrt{2}q \sin\theta)^2 \right] (\sqrt{s} p A_5 + 2p_0 q \cos\theta A_8) + \frac{l \cdot p}{M_T^2} (\sqrt{s} p A_1 - 2q l_0 \cos\theta A_2) \right\},
\end{aligned} \tag{B4}$$

and $M_{-\lambda, -\mu} = (-1)^{\lambda-\mu} M_{\lambda, \mu}$, with the notation

$$\begin{aligned}
q &= \frac{1}{2}(s - 4\mu^2)^{1/2}; \quad p = \frac{1}{2\sqrt{s}} [s - (M_T - m)^2]^{1/2} [s - (M_T + m)^2]^{1/2}, \\
p_0 &= \frac{s + m^2 - M_T^2}{2\sqrt{s}}, \quad l_0 = \frac{s + M_T^2 - m^2}{2\sqrt{s}}, \quad l \cdot p = \frac{s - M_T^2 - m^2}{2},
\end{aligned}$$

and $\frac{1}{4}(t - u) = pq \cos\theta$.

The invariant amplitudes in the Born approximation are

$$\begin{aligned}
A_{1, \text{Born}}^{t+u} &= -[(s - u)t + (M_T^2 - \mu^2)(m^2 - \mu^2)]X(t) - (t - u), \quad A_{2, \text{Born}}^{t+u} = [(s - u)t + (M_T^2 - \mu^2)(m^2 - \mu^2)]X(t) + (t - u), \\
A_{3, \text{Born}}^{t+u} &= [(t - u) - \frac{3}{2}s + \frac{1}{2}(M_T^2 + m^2) + 4\mu^2]X(t) - (t - u), \\
A_{4, \text{Born}}^{t+u} &= [\frac{3}{2}s - \frac{1}{2}(M_T^2 - m^2) - 4\mu^2 - \frac{1}{2}(t - u)]X(t) + (t - u), \\
A_{5, \text{Born}}^{t+u} &= -[\frac{1}{2}(t - u) + m^2]X(t) - (t - u), \quad A_{6, \text{Born}}^{t+u} = -[\frac{1}{2}(t - u) + M_T^2]X(t) + (t - u), \\
A_{7, \text{Born}}^{t+u} &= \frac{1}{2}[(t - u) - s + M_T^2 - m^2]X(t) - (t - u), \quad A_{8, \text{Born}}^{t+u} = -\frac{1}{2}(s - M_T^2 - m^2)X(t) + (t - u),
\end{aligned} \tag{B5}$$

where

$$X(t) = \frac{X}{t - m_\rho^2} \quad \text{and} \quad X = \frac{g_{A_2 \rho \pi} g_{\omega \rho \pi}}{8\mu^3}; \tag{B6}$$

$$A_{1, \text{Born}}^s = \beta_1 \frac{(t - u)}{2} Y(s), \quad A_{2, \text{Born}}^s = \alpha Y(s), \quad A_{3, \text{Born}}^s = -\delta \frac{(t - u)}{2} Y(s), \tag{B7}$$

$$A_{4, \text{Born}}^s = -\beta_2 Y(s), \quad A_{6, \text{Born}}^s = -\gamma Y(s), \quad A_{5, \text{Born}}^s = A_{7, \text{Born}}^s = A_{8, \text{Born}}^s = 0,$$

where α , β_1 , β_2 , γ , and δ were defined in Sec. II and

$$Y(s) = \frac{Y}{s - m_\rho^2}, \quad \text{with} \quad Y = g_{A_2 \omega \rho} g_{\rho \pi \pi}. \tag{B8}$$

The dual representation reads

$$\begin{aligned}
R_1^{(t+u)} &= -\frac{X(\alpha_t - \alpha_u)}{(2 - \alpha_t - \alpha_u)} [m_\rho^2(2s + m_\rho^2 - \Sigma) + (M_T^2 - \mu^2)(m^2 - \mu^2)], \\
R_2^{(t+u)} &= X \left[m_\rho^2(2s + m_\rho^2 - \Sigma) + (M_T^2 - \mu^2)(m^2 - \mu^2) - \frac{s}{\epsilon'} \frac{(1 - \alpha_t)(1 - \alpha_u)}{(2 - \alpha_t - \alpha_u)} \right], \\
R_3^{(t+u)} &= \frac{X(\alpha_t - \alpha_u)}{(2 - \alpha_t - \alpha_u)} [2m_\rho^2 + 3\mu^2 - \frac{1}{2}(s + \Sigma)], \\
R_4^{(t+u)} &= X \left[s + m^2 - m_\rho^2 - 3\mu^2 - \frac{2(1 - \alpha_t)(1 - \alpha_u)}{(2 - \alpha_t - \alpha_u)} \left(\frac{1}{\epsilon'} + \frac{M_T^2 + m^2}{4 - \alpha_t - \alpha_u} \right) \right], \\
R_5^{(t+u)} &= -\frac{X(\alpha_t - \alpha_u)}{(2 - \alpha_t - \alpha_u)} \left[\frac{1}{2}(s - \Sigma) + m^2 + m_\rho^2 \right], \\
R_6^{(t+u)} &= -X \left[\frac{1}{2}(s - \Sigma) + M_T^2 + m_\rho^2 - \frac{2(1 - \alpha_t)(1 - \alpha_u)}{(2 - \alpha_t - \alpha_u)} \left(\frac{1}{\epsilon'} + \frac{M_T^2 + m^2}{4 - \alpha_t - \alpha_u} \right) \right], \\
R_7^{(t+u)} &= \frac{X(\alpha_t - \alpha_u)}{(2 - \alpha_t - \alpha_u)} (s + m_\rho^2 - m^2 - \mu^2), \quad R_8^{(t+u)} = -X \frac{1}{2} (s - M_T^2 - m^2); \\
R_1^{(s)} &= Y\beta_1 \frac{(t-u)}{2} \frac{(3-\epsilon)}{(2-\alpha_t-\alpha_u)}, \quad R_2^{(s)} = Y\alpha, \quad R_3^{(s)} = -Y\delta \frac{(t-u)}{2} \frac{(3-\epsilon)}{(2-\alpha_t-\alpha_u)}, \\
R_4^{(s)} &= -Y\beta_2, \quad R_6^{(s)} = -Y\gamma, \quad R_5^{(s)} = R_7^{(s)} = R_8^{(s)} = 0;
\end{aligned} \tag{B9}$$

with

$$\Sigma = M_T^2 + m^2 + 2\mu^2, \quad \epsilon = \alpha_s + \alpha_t + \alpha_u. \tag{B11}$$

*Research supported in part by the Israel Commission for Basic Research.

¹A good source for the relevant material is the *Proceedings of the International Conference on Meson Resonances and Related Electromagnetic Phenomena, Bologna, 1971*, edited by R. H. Dalitz and A. Zichichi (Editrice Compositori, Bologna, Italy).

²For reviews on the present status of knowledge on these couplings and the validity of the relevant symmetry schemes see N. P. Samios, M. Goldberg, and B. T. Meadows, *Rev. Mod. Phys.* **46**, 49 (1974); H. Pilkuhn, W. Schmidt, A. D. Martin, C. Michael, F. Steiner, B. R. Martin, M. M. Nagels, and J. J. de Swart, *Nucl. Phys.* **B65**, 460 (1973); J. Rosner, *Phys. Rep.* **11C**, 190 (1974).

³Experimental work on $A_2 \rightarrow \omega\pi\pi$ has been reported by:

- (a) C. Defoix *et al.*, *Phys. Lett.* **43B**, 141 (1973) [$R_\omega = \Gamma(A_2 \rightarrow \omega\pi\pi)/\Gamma(A_2 \rightarrow \rho\pi) = 0.23 \pm 0.10$]; (b) V. Chaloupka *et al.*, *ibid.* **44B**, 211 (1973) ($R_\omega = 0.10 \pm 0.05$); (c) J. Díaz *et al.*, *Phys. Rev. Lett.* **32**, 260 (1974) ($R_\omega = 0.28 \pm 0.09$); (d) U. Karshon *et al.*, *ibid.* **32**, 852 (1974) ($R_\omega = 0.29 \pm 0.08$ for A_2^0 and $R_\omega = 0.10 \pm 0.04$ for A_2^\pm); (e) LBL Group A, quoted by S. M. Flatte, in *Proceedings of the XVI International Conference on High Energy Physics, Chicago-Batavia, Ill., 1972*, edited by J. D. Jackson and A. Roberts (NAL, Batavia, Ill., 1973), Vol. 1, p. 137 ($R_\omega = 0.07^{+0.04}_{-0.02}$).

⁴Experimental work on $f \rightarrow 4\pi$ has been reported by: (a) G. Ascoli *et al.*, *Phys. Rev. Lett.* **21**, 1712 (1968) [$R_{4\pi} = f^0 \rightarrow \pi^+\pi^-\pi^+\pi^-/f^0 \rightarrow \pi^+\pi^-\pi^+\pi^- \approx 10\%$]; (b) M. Bardadin-Otwinowska *et al.*, *Phys. Rev. D* **4**, 2711 (1971) [$R_{4\pi} = (3.3 \pm 4.5)\%$]; (c) B. Y. Oh *et al.*, *ibid.* **1**, 2494 (1970) [$R_{4\pi} = (7 \pm 2)\%$]; (d) W. M. Bugg *et al.*, *ibid.* **7**, 3264 (1973) ($R_{4\pi} < 4\%$ with 90% confidence); (e) J. C. Anderson

et al., *Phys. Rev. Lett.* **31**, 562 (1973) [$R_{4\pi} = (5.5 \pm 1.0)\%$];

(f) J. Louie *et al.*, *Phys. Lett.* **48B**, 385 (1974) [$R_{4\pi} = (6.5 \pm 1.7)\%$]; (g) M. J. Emms *et al.*, *Nucl. Phys.* **B96**, 155 (1975) [$R_{4\pi} = 3.5 \pm 0.8\%$]. The last entry is not yet included in the world average of Ref. 16.

⁵A. Capella, B. Diu, J. M. Kaplan, and D. Schiff, *Lett. Nuovo Cimento* **1**, 655 (1969).

⁶P. Carruthers and E. Lasley, *Phys. Rev. D* **1**, 1204 (1970).

⁷N. Levy and P. Singer, *Phys. Rev. D* **3**, 1028 (1971).

⁸P. Aurenche, *Phys. Rev. D* **9**, 1514 (1974).

⁹N. Levy and P. Singer, *Phys. Rev. D* **4**, 2177 (1971).

¹⁰The couplings defined in (1) differ from those defined in Eq. (7) of Ref. 9 and are, in fact, equivalent to the primed couplings of that article. There are several misprints in the table and some of the equations of Ref. 9; the interested reader is therefore advised to use the expressions of the present paper. The value given in Ref. 9 for $\Gamma(f \rightarrow \omega\gamma)$ is superseded by the one given in Table II of this article, in whose calculation we used more recent values for the constants involved.

¹¹E. S. Abers and V. L. Teplitz, *Phys. Rev. Lett.* **22**, 909 (1969); *Phys. Rev. D* **1**, 624 (1970).

¹²B. Renner, *Nucl. Phys.* **B30**, 634 (1971).

¹³G. Veneziano, *Nuovo Cimento* **57A**, 190 (1968).

¹⁴See, e.g., V. Barger, in *Proceedings of the XVII International Conference on High Energy Physics, London, 1974*, edited by J. R. Smith (Rutherford Laboratory, Chilton, Didcot, Berkshire, England), p. I-913.

¹⁵F. J. Gilman and H. Harari, *Phys. Rev.* **165**, 1803 (1968).

¹⁶Particle Data Group, *Phys. Lett.* **50B**, 1 (1974).

¹⁷In a recent paper by D. Parashar and P. N. Dobson [*Phys. Rev. D* **12**, 77 (1975)], the width for $A_2 \rightarrow (\rho\pi)$

$\rightarrow \omega \pi \pi$ is calculated to be ~ 35 MeV. This term corresponds to our $\Gamma_{\text{Bom}}^{t+u}$ from Table I. We found that the $\sim 10^3$ discrepancy is due to: (a) the use by Parashar and Dobson of an $A_2 \rho \pi$ coupling which is ~ 3 times larger than the experimental one; (2) an unfortunate error of $\sim 10^2$ in their phase-space calculation.

¹⁸D. Parashar, Phys. Rev. D 10, 3884 (1974).

¹⁹L. Bányai and V. Rittenberg, Nucl. Phys. B15, 199 (1970).

²⁰E. Golowich, Phys. Rev. D 10, 3861 (1974).

²¹A. Bramòn and M. Greco, Lett. Nuovo Cimento, 2, 522 (1971).

²²B. Schremp-Otto, F. Schrempp, and T. F. Walsh, Phys. Letters 36B, 463 (1971).

²³H. Kleinert, L. P. Staunton and P. H. Weisz, Nucl. Phys. B38, 87 (1972).

²⁴G. Schierholz and K. Sundermeyer, Nucl. Phys. B40, 125 (1972).

²⁵Using a dispersion relation for the amplitude for $\pi^0 + \pi^0 \rightarrow \gamma + \gamma$ scattering and some additional assump-

tions, G. M. Radutskii has obtained sum rules for $g_{f\gamma\gamma}$ and $g_{A_2\gamma\gamma}$ similar to those presented in Eqs. (22), (23) (Zh. Eksp. Teor. Fiz. Pis'ma 6, 911 (1962) [JETP Lett. 6, 336 (1967)] and Yad. Fiz. 8, 115 (1968) [Sov. J. Nuc. Phys. 8, 65 (1969)]). See also L. V. Fil'kov, Zh. Eksp. Teor. Fiz. Pis'ma Red. 5, 192 (1967) [JETP Lett. 5, 153 (1967)]. Unfortunately, the calculations in these articles are plagued with errors, preventing the inclusion of their predictions in Table II.

²⁶S. B. Berger and B. T. Feld, Phys. Rev. D 8, 3875 (1973).

²⁷D. Faiman, H. J. Lipkin, and H. R. Rubinstein, Phys. Lett. 59B, 269 (1975).

²⁸We note that the near equality between our couplings and Renner's (Ref. 12) is not completely preserved for the electromagnetic couplings. While Renner uses vector-meson dominance to go from TVV to the electromagnetic coupling, our $TV\gamma$ and $T\gamma\gamma$ vertices are obtained as a limiting case from the general TVV vertex.